Liver Imaging Today

Tobias Heye, M.D.[1]; Mustafa R. Bashir, M.D.[2]

[1]Department of Radiology, University Hospital Basel, Switzerland
[2]Department of Radiology, Duke University Medical Center, NC, USA

Introduction

Liver disease is a global burden with a growing incidence and prevalence. The World Health Organization recently estimated that there are 800,000 cirrhosis-related deaths per year world-wide [1]. Chronic liver disease has a great impact on public health care costs with therapeutic options ranging from antiviral treatment for viral hepatitis to orthotopic liver transplant for end stage cirrhosis. A variety of pathogens, which can be toxic, viral, metabolic or autoimmune in nature, can induce fibrosis which may progress to cirrhosis if the disease is not detected and treated. An estimated 150 million people world-wide are chronically infected with hepatitis C virus, approximately 350,000 people die due to hepatitis C related liver disease [2]. Liver fibrosis may be reversible at an early stage, which indicates the importance of screening and detection of liver disease. Many forms of liver fibrosis and cirrhosis especially secondary to viral hepatitis increase the risk for the development of liver cancer, namely hepatocellular carcinoma.

Non-alcoholic steatohepatatis is emerging as a major pathway into chronic liver disease and is closely related to other metabolic disease entities such as diabetes and morbid obesity. The incidence and prevalence of these diseases has risen steadily over recent years.

In a clinical context, liver disease is often reflected by a combination of several contributing factors, fibrosis, hepatic steatosis and iron overload, each with different forms of manifestations. Although these diseases are considered 'diffuse', actual hepatic parenchymal involvement by any of these can be irregular and patchy, leaving other parenchymal areas unaffected.

Clinical management of patients with diffuse liver disease requires tools to accurately detect and classify the various forms of liver disease. Even with decades of experience in imaging, liver biopsy and the histological workup of the specimens have traditionally been the reference standard in the characterization of liver disease [3]. However, biopsy is prone to sampling errors if less affected parenchyma is sampled and may not reflect the true disease severity and distribution in a particular organ due to the variance in the heterogeneous pattern of histological changes on a macroscopic scale [4, 5]. Biopsy, associated with the risks of an invasive procedure, is employed for disease detection and staging, but periodically repeated biopsy is not a practical

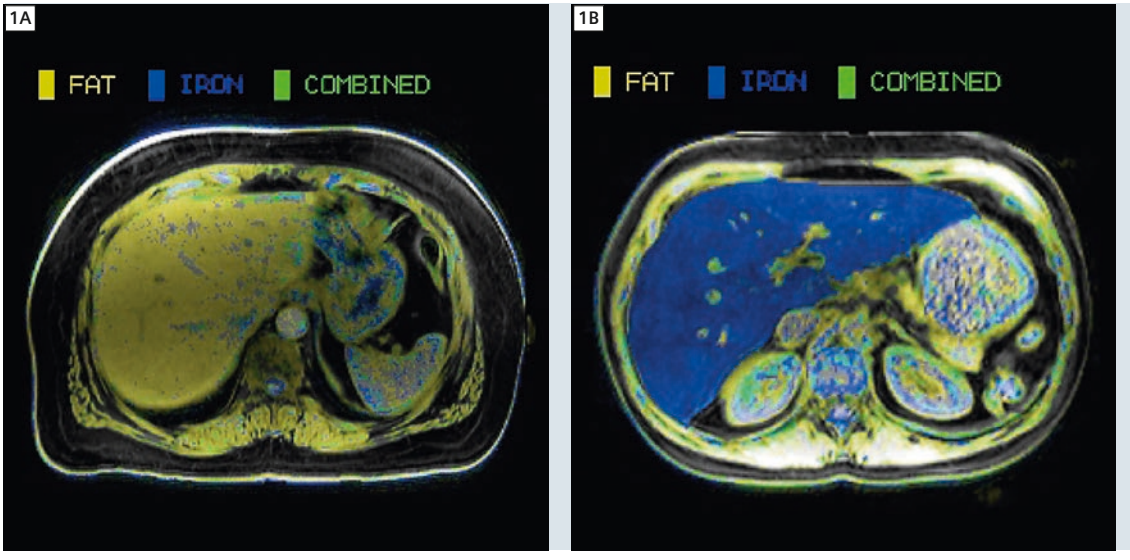

1 Results of the Screening Dixon technique which produces color coded maps to visualize the distribution of detected abnormal metabolites in two different clinical examples. **(1A)** A patient with diffuse hepatic steatosis as indicated by the yellow hue. **(1B)** A patient with diffuse iron overload as marked by blue overlay to the affected liver.

method for disease monitoring. Additionally, given its attendant risks and costs, biopsy is only performed in patients in whom liver disease is strongly suspected, and is not suitable for evaluating those patients with only mild or questionable symptoms. Thus, there has been great interest in non-invasive methods to assess diffuse liver disease, and imaging modalities, in particular magnetic resonance imaging (MRI), have evolved as potential tools to measure certain biomarkers.

Liver MRI offers a variety of methods to detect and quantify parenchymal changes which occur in chronic liver disease [6, 7]. In contrast to liver biopsy, liver MRI allows for assessment and evaluation of the entire liver volume by means of quantitative measurements and color coded maps which reflect the geographical disease distribution. Quantification of excessive fat and iron deposition was shown to be accurate as demonstrated by many studies in the literature [8, 9]. The characterization of focal liver lesions and determination of treatment options for hepatocellular carcinoma is a well-established clinical application of liver MRI, and this use will grow as the prevalence of chronic liver disease increases [10]. The detection and accurate classification of liver fibrosis and cirrhosis remains challenging, despite the usefulness of liver MRI in the aforementioned scenarios [7].

While liver MRI may soon provide a comprehensive evaluation of liver disease it is a complex technique requiring highly trained personnel, cooperative patients and optimized scanning conditions to produce diagnostic images acceptable for clinical interpretation. MRI must compete with other imaging modalities, sonography and computed tomography (CT) in categories such as availability, cost, acquisition time, robustness, reproducibility, patient acceptance, and comfort. In particular, it has been advocated that MRI needs to close the gap in acquisition time compared to CT; simultaneously methods should be employed to standardize the image acquisition workflow, improve reproducibility of a quantitative imaging protocol, and reduce the time spent performing redundant data acquisition or preparatory steps [11]. However, in terms of diagnostic performance, lack of ionizing radiation compared with CT, and the variety of tissue contrasts available, MRI has several clear advantages. In the following article we will discuss new methods which address MRI related issues like artifacts and breathing motion while improving image quality and spatial resolution, offer fast automated screening techniques for the detection of parenchymal changes, and optimize the imaging workflow to decrease overall acquisition time.

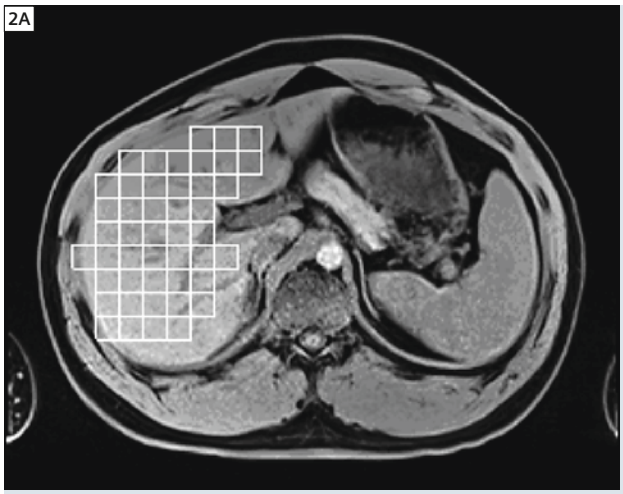

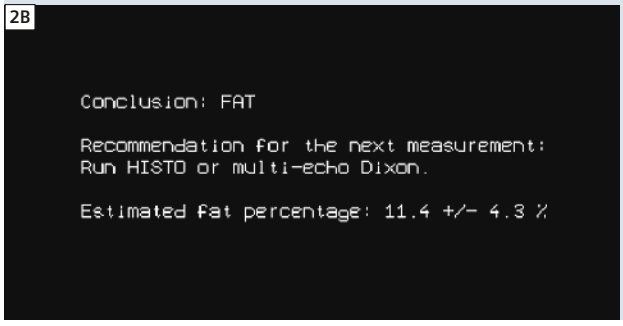

2 Example of the Screening Dixon segmentation algorithm which identifies large portions of the liver and the automated conclusion given by the dual signal intensity ratio calculation (In-phase/Opposed-phase and Fat-Only/Water-Only data sets) in a volunteer. **(2A)** Segmentation result, **(2B)** automated conclusion.

Liver imaging

A modern liver imaging protocol must accomplish at least two main goals. The presence of diffuse liver disease, fat, iron deposition and possibly fibrosis/cirrhosis should be detected and ideally quantified, even if not expected at the time that the examination is initiated. Additionally, focal hepatic lesions, in particular in the setting of cirrhosis, must be characterized to allow for classification into benign entities, such as simple cysts, hemangiomas, focal nodular hyperplasias (FNH) or adenomas versus malignant hepatic tumors like hepatocellular carcinoma, cholangiocarcinoma or metastatic disease. These tasks must be accomplished within a reasonable amount of time without compromise in image quality or obtainable information. A number of methodologies have become recently available which provide automated diagnosis of diffuse liver disease, higher spatial resolution imaging, and automated workflows.

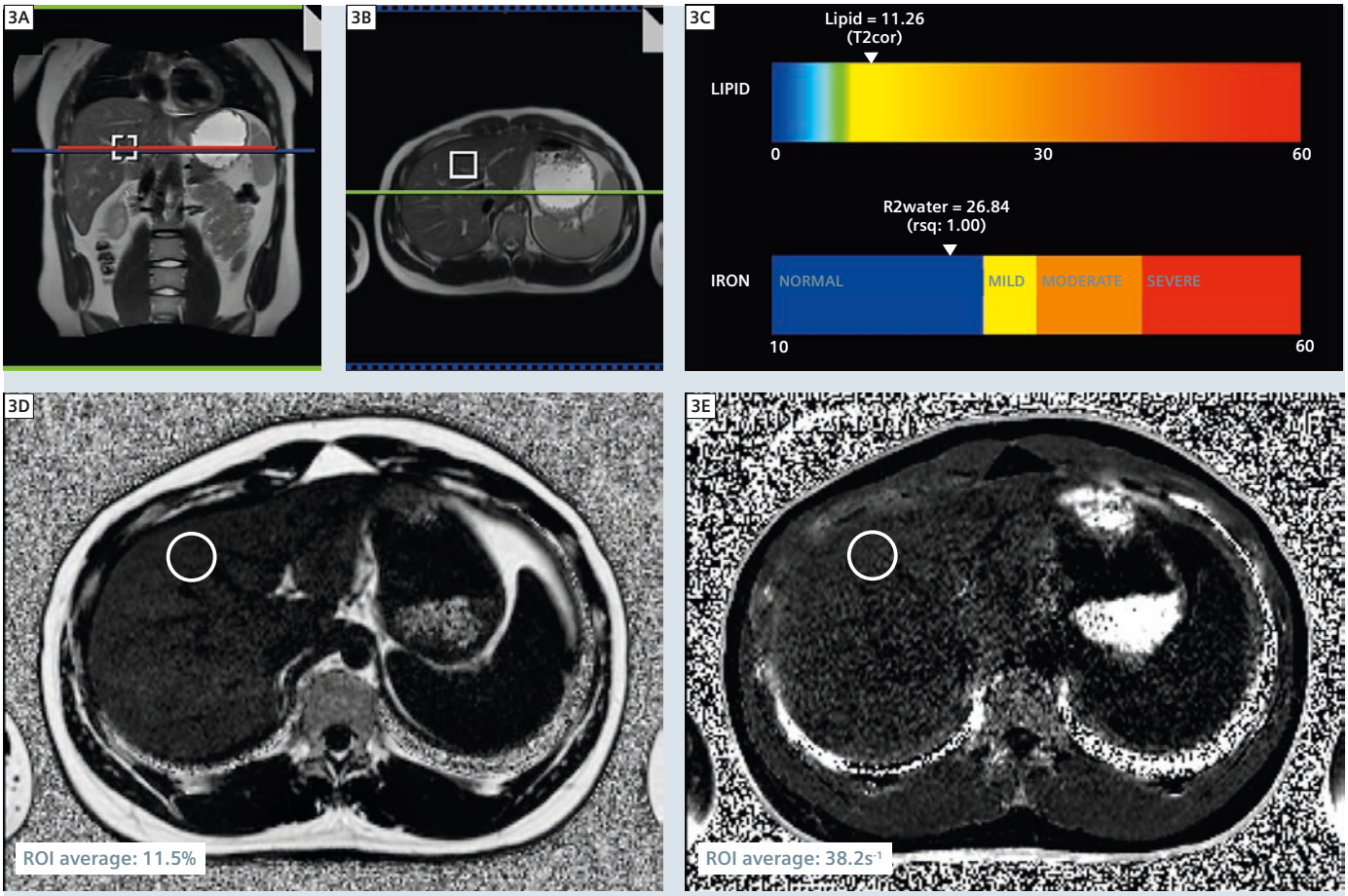

3 Quantification results from the same volunteer as in Fig. 2. **Top:** HISTO **(3A, B)** voxel positioning, **(3C)** quantification results in a graphical norm range display. **Bottom:** Multi-echo Dixon **(3D)** fat percentage map, **(3E)** R2* map.

Screening Dixon

Fat and water separation can be realized by 3D In- and Opposed-Phase T1-weighted data acquisition with two-point Dixon reconstruction. This 3D gradient-echo imaging sequence produces four sets of images with In-/Opposed-Phase, Water-Only and Fat-Only depiction. The Water-Only image set can further be employed as a standard pre-contrast fat-suppressed sequence, one of the standard in a liver MRI protocol with contrast material application [12]. The two-point Dixon method offers visual, qualitative assessment of hepatic steatosis but the acquired data allow for a semi-quantitative estimation of fat deposition as well as iron overload [13, 14]. This pulse sequence provides two essential image sets (In- and Opposed-Phase and pre-contrast T1) in a single breath-hold. The Screening Dixon method represents a two-point Dixon technique with an additional liver sampling algorithm that automatically segments large portions of the liver. Within a large volume of the segmented liver, dual signal intensity ratios from In-phase/Opposed-phase and Fat-Only/Water-Only data sets are calculated by the algorithm to produce an assessment regarding the presence of diffuse liver disease. The result of the algorithm (normal, fat, iron, or combined disease) can be coupled with a recommendation to perform a dedicated quantitative sequence for the detected abnormal metabolite (e.g. iron quantification sequence) [13, 15].

Hence, the Screening Dixon technique offers an automated approach to diffuse liver disease but simultaneously allows for a quantitative MRI protocol tailored to the individual patient. Instead of performing a time consuming all-in-one MR imaging protocol that comprises any type of quantification, the Screening Dixon methods stratifies protocol steps in a way that only essential quantitative sequences are acquired, potentially reducing overall acquisition time compared with an exam which performs quantification unnecessarily (Figs. 1, 2). Notably, although this method can provide estimates of proton density fat fraction (PDFF) and R_2* (a surrogate for iron concentration), these are not corrected for a variety of potentially confounding factors, and should be confirmed by a dedicated quantification sequence when abnormal. Even so, this algorithm performs well for the task of detecting diffuse steatosis/siderosis [16].

Fat and iron quantification

R2* and PDFF can be quantified in two different ways. Multi-echo, T2 corrected, single breath-hold spectroscopy (HISTO) gives highly reproducible values from a single voxel [17]. Multi-echo 3D gradient echo (VIBE) imaging, with Dixon reconstruction and correction for T2* as well as the multi-spectral nature of fat, allows quantification with good spatial resolution [18].
Figure 3 shows quantification results from the same volunteer as in Fig. 2. The results are consistent and support the initial Screening Dixon estimation.

CAIPIRINHA

There are two distinct time points within a contrast enhanced liver MRI protocol which are crucial in the acquisition of diagnostic images. Hepatic arterial phase imaging is the mainstay in the detection of hepatocellular carcinoma [18].Here, accurate timing is important [22]. The images may be acquired as a multi-arterial phase to improve temporal resolution [17]. A 'late phase', whether the vascular equilibrium phase obtained with extracellular contrast agents or the hepatocyte phase obtained with hepatobiliary agents, can differentiate lesions based on their contrast retention behavior. For both elements within a liver MRI protocol, a compromise must be made between achievable image resolution and acquisition time. This conflict is even more challenging for single breath-hold/ multiple arterial phase imaging. The duration of a breath-hold remains the limiting factor in contrast enhanced liver imaging, and a sequence must balance the two factors; sufficient spatial resolution within a reasonable acquisition time. The evolution of parallel imaging techniques has allowed multiple acquisitions within the arterial phase time window to reliably capture the late hepatic arterial phase, a critical image for hepatocellular carcinoma imaging. However, 20-25 second breath-holds remain challenging for some patients. Hepatobiliary phase imaging is ideally done using high spatial resolution to utilize the diagnostic information derived from hepatocyte specific contrast agent for all liver abnormalities, in particular for smaller otherwise indeterminate lesions (> 1 cm lesion diameter). Although the time window for the hepatobiliary phase is wider compared to arterial phase imaging, the achievable spatial resolution is similarly limited by the duration of a breath-hold which may be even shorter at the end of an examination due to developing fatigue of the patient. Patients with impaired or poor breath-holding capabilities may render any breath-hold sequence acquisition non-diagnostic if the acquisition time exceeds their capabilities. Further increasing standard parallel imaging acceleration, however, decreases the signal-to-noise ratio (SNR) and induces image artifacts.

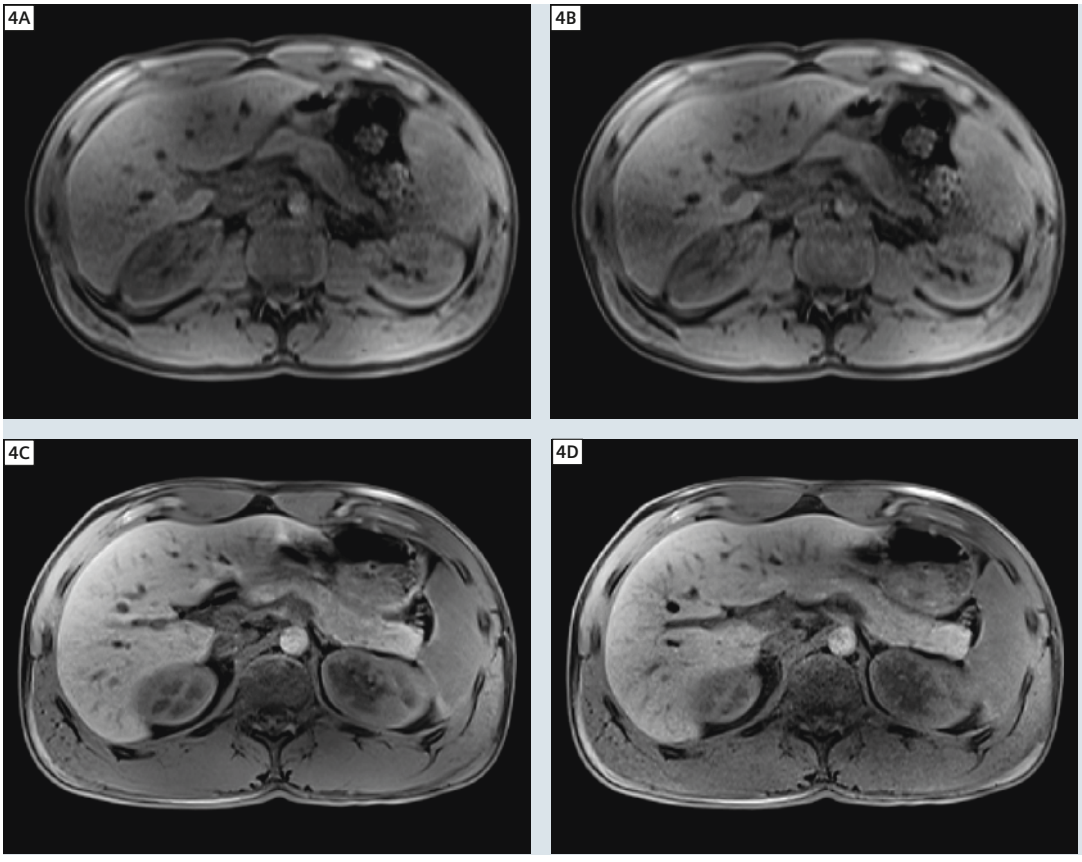

4 Comparison of standard VIBE acquisition with iPAT acceleration to acceleration with CAIPIRHINA and higher-order acceleration factors in a volunteer without intravenous contrast. Please note how acquisition time and/or spatial resolution can be modulated by incorporating CAIPIRHINA.
Triple phase imaging, slice thickness 5 mm, matrix 256 × 128:
(4A) iPAT, acceleration factor 2: acquisition time 28 seconds for three phases.
(4B) CAIPIRINHA, acceleration factor 2 × 3: acquisition time 11 seconds for three phases.
Single phase imaging, slice thickness 3 mm, matrix 320 × 195:
(4C) iPAT, acceleration factor 2: acquisition time 20 seconds.
(4D) CAIPIRINHA, acceleration factor 2 x 2: acquisition time 13 seconds.

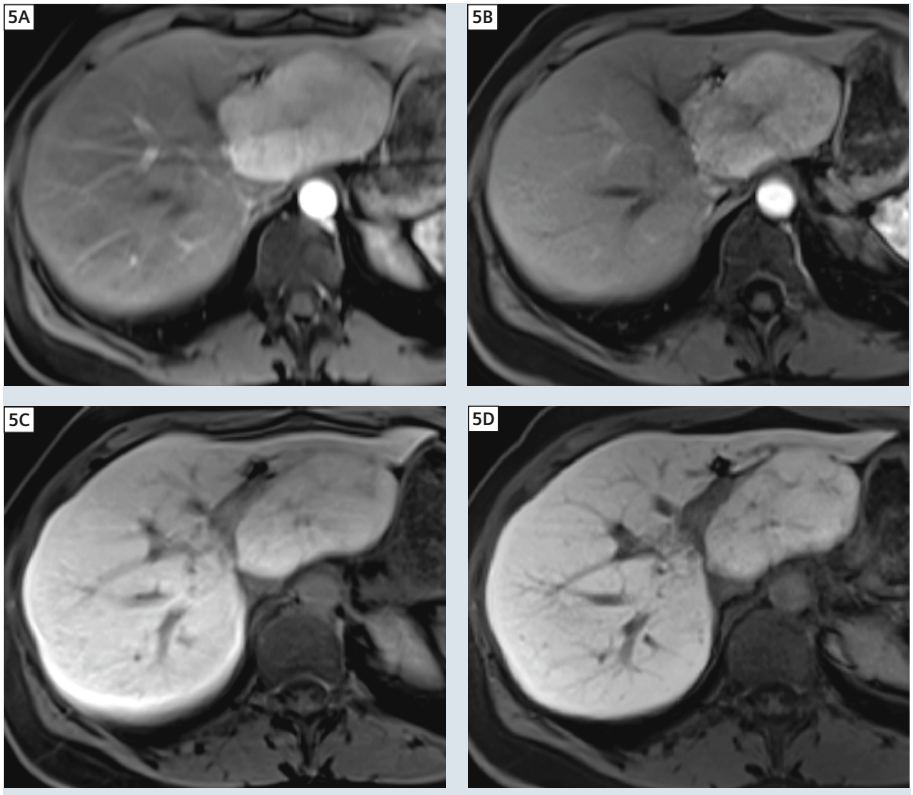

5 Triple arterial phase imaging:
(5A) iPAT, acceleration factor 2: matrix 256 × 115, spatial resolution 1.3 × 2.8 × 5 mm, acquisition time 29 seconds for three phases.
(5B) CAIPIRINHA, acceleration factor 2 × 2: matrix 256 × 156, spatial resolution 1.3 × 1.8 × 5 mm, acquisition time 26 seconds for three phases.
Hepatobiliary phase imaging:
(5C) iPAT, acceleration factor 2: matrix 256 × 192, spatial resolution 1.3 × 1.8 × 4 mm, acquisition time 22 seconds.
(5D) CAIPIRINHA, acceleration factor 2 × 3: matrix 288 × 216, spatial resolution 1.2 × 1.6 × 4 mm, acquisition time 12 seconds.
Two examinations utilizing iPAT and CAIPIRINHA acceleration and gadoxetate disodium in a patient with a focal liver lesion characterized as focal nodular hyperplasia (FNH) based on arterial and hepatobiliary phase imaging. Comparison between standard iPAT and CAIPIRHINA acquisition reveals improved contrast, sharpness and detail based on increased spatial resolution. Acquisition time was also decreased in the hepatobiliary phase (5D), eliminating the breathing motion artifacts seen in (5C).

CAIPIRINHA (Controlled Aliasing in Parallel Imaging Results in Higher Acceleration), a new parallel imaging technique differs in the *k*-space sampling pattern compared to standard acceleration techniques and is more efficient in using the coil sensitivities [21]. Undersampling is performed in both the phase and partition directions, allowing for a higher acquisition matrix and improved image resolution. This provides dramatic improvements in spatial resolution for the same breath-hold times, and can be optimized to provide a combination of high spatial resolution and reduced breath-hold duration (Figs. 4, 5).

Workflow – Abdomen Dot Engine

MRI data acquisition is time consuming, and the considerably longer examination times (compared to CT) must be justified by added benefits to patient care. Total examination time is composed of time spent acquiring image data and time spent performing a variety of setup tasks, including patient positioning and pulse sequence preparation. In liver MRI, preparatory tasks have been shown to consume more time than image acquisition, as such there is substantial opportunity for improvement in addressing the efficiency of performing these tasks [19]. This leads to operator dependent workflow, inconsistent image quality, and prolonged examination times. Additional patient specific factors further influence the achievable image quality and overall examination time, for example patients vary in their breath-holding capabilities and may fatigue throughout an examination. Adjustment of the imaging strategy, breath-hold versus free breathing, triggered imaging versus a shortened, fast imaging protocol may be necessary to accommodate individual differences. Additionally, many of the pulse sequence preparatory tasks are redundant and therefore offer opportunities for automation or a guided standardized setup. The current MRI acquisition workflow can be rendered more efficient thus reducing overall room time.
The Abdomen Dot Engine is an approach that incorporates various strategies to optimize and standardize a complex abdominal MRI protocol. It allows for automatic detection and positioning of an individualized field-of-view (FOV) based on localizer images, can stratify a protocol into patient specific breathing capabilities and provides tools such as automatic bolus timing for dynamic scanning [20]. A liver MRI protocol, for example can be standardized and partitioned into its typical elements (pre-contrast, multiple arterial, portal venous, and equilibrium phases), so that key settings such as delay times between each element can be configured by the user through an interface that offers an overview of all protocol steps (Fig. 6).
A standardized and guided workflow for MRI examinations is needed to release the operator from redundant tasks, such as defining patient-specific sequence parameters, and allowing him or her to focus on global protocol strategies. Furthermore, the consistency of image quality across studies may be improved, and the risk of rescanning a sequence or the entire protocol may be reduced, increasing the robustness of the modal-

6 Example of the Abdomen Dot Engine user interface showing the guidance view that allows global planning of delay times within a dynamic contrast enhanced liver MRI protocol.

ity. Additionally, multiple scan types which differ by only a few minor components (e.g., with or without MR Cholangiopancreatography (MRCP), with or without diffusion-weighted imaging) can be combined into a single, efficient protocol with a few key decision points, reducing redundancy and allowing for simpler base protocol maintenance and modification when necessary.

Summary

MRI examinations face serious competition compared to sonography and CT when categories such as robustness, acquisition time, patient comfort and health care costs are considered. An abundance of information may be acquired through high resolution imaging and dedicated quantitative MRI sequences, but images and measurements should be reproducible and reliable in their diagnostic value. The redundancy of preparatory steps for the operator within an MRI protocol is an opportunity for more efficient and less time consuming imaging. In addition, the image acquisition process can be improved by means of faster imaging at higher resolution with the implementation of new parallel imaging acceleration techniques, to reduce the risk of motion in patients with limited breath-hold capabilities. Intelligent imaging protocols, which self-optimize during the course of the examination or use initial pulse sequences to tailor subsequent sequence selection, can provide faster and more efficient examinations, which include quantitative data when appropriate. Combining all of the described improvements may equip liver MRI examinations with sufficient tools to remain unique in delivering disease specific quantitative data while expanding their diagnostic value.

References

1 The global burden of disease: 2004 update. World Health Organization, 2004.
2 Hepatitis C. Fact sheet N°164: World Health Organization, July 2012.
3 Angelucci E, Brittenham GM, McLaren CE, et al. Hepatic iron concentration and total body iron stores in thalassemia major. The New England journal of medicine. 2000;343(5):327-31.
4 Rockey DC, Caldwell SH, Goodman ZD, Nelson RC, Smith AD, American Association for the Study of Liver D. Liver biopsy. Hepatology. 2009;49(3):1017-44.
5 Villeneuve JP, Bilodeau M, Lepage R, Cote J, Lefebvre M. Variability in hepatic iron concentration measurement from needle-biopsy specimens. J Hepatol. 1996;25(2):172-7.
6 Boll DT, Merkle EM. Diffuse liver disease: strategies for hepatic CT and MR imaging. Radiographics. 2009;29(6):1591-614.
7 Bonekamp S, Kamel I, Solga S, Clark J. Can imaging modalities diagnose and stage hepatic fibrosis and cirrhosis accurately? J Hepatol. 2009;50(1):17-35.
8 Meisamy S, Hines CD, Hamilton G, et al. Quantification of hepatic steatosis with T1-independent, T2-corrected MR imaging with spectral modeling of fat: blinded comparison with MR spectroscopy. Radiology. 2011;258(3):767-75.
9 Yokoo T, Shiehmorteza M, Hamilton G, et al. Estimation of hepatic proton-density fat fraction by using MR imaging at 3.0 T. Radiology. 2011;258(3):749-59.
10 Cruite I, Schroeder M, Merkle EM, Sirlin CB. Gadoxetate disodium-enhanced MRI of the liver: part 2, protocol optimization and lesion appearance in the cirrhotic liver. AJR American journal of roentgenology. 2010;195(1):29-41.
11 Bashir MR, Dale BM, Gupta RT, Horvath JJ, Boll DT, Merkle EM. Gradient shimming during magnetic resonance imaging of the liver: comparison of a standard protocol versus a novel reduced protocol. Investigative radiology. 2012;47(9):524-9.
12 Ringe KI, Husarik DB, Sirlin CB, Merkle EM. Gadoxetate disodium-enhanced MRI of the liver: part 1, protocol optimization and lesion appearance in the noncirrhotic liver. AJR American journal of roentgenology. 2010;195(1):13-28.
13 Bashir MR, Merkle EM, Smith AD, Boll DT. Hepatic MR imaging for in vivo differentiation of steatosis, iron deposition and combined storage disorder: single-ratio in/opposed phase analysis vs. dual-ratio Dixon discrimination. European journal of radiology. 2012;81(2):e101-9.
14 Boll DT, Marin D, Redmon GM, Zink SI, Merkle EM. Pilot study assessing differentiation of steatosis hepatis, hepatic iron overload, and combined disease using two-point dixon MRI at 3 T: in vitro and in vivo results of a 2D decomposition technique. AJR American journal of roentgenology. 2010;194(4):964-71.
15 Bashir MR, Dale BM, Merkle EM, Boll DT. Automated liver sampling using a gradient dual-echo Dixon-based technique. Magnetic resonance in medicine : official journal of the Society of Magnetic Resonance in Medicine / Society of Magnetic Resonance in Medicine. 2012;67(5):1469-77.
16 Bashir MR, Zhong X, Dale BM, Gupta RT, Boll DT, Merkle EM. Automated patient-tailored "Screening" of the liver for diffuse steatosis and iron overload using MRI. Am J Roentgenol; in press.
17 Pineda N, Sharma P, Xu Q, et al. Measurement of Hepatic Lipid: High-Speed T2-Corrected Multi-echo Acquisition at 1H MR Spectroscopy – A Rapid and Accurate Technique. Radiology 2009, 252(2):568-76.
18 Zhong X, Nickel MD, Kannengiesser SAR, Dale B, Kiefer B, Bashir M. Fat and Iron Quantification Using a Multi-Step Adaptive Fitting Approach with Multi-Echo GRE Imaging. Proc. Intl. Soc. Magn. Reson. Med 2013, 21:401.
19 Willatt JM, Hussain HK, Adusumilli S, Marrero JA. MR Imaging of hepatocellular carcinoma in the cirrhotic liver: challenges and controversies. Radiology. 2008;247(2):311-30.
20 Mori K, Yoshioka H, Takahashi N, et al. Triple arterial phase dynamic MRI with sensitivity encoding for hypervascular hepatocellular carcinoma: comparison of the diagnostic accuracy among the early, middle, late, and whole triple arterial phase imaging. AJR Am J Roentgenol. 2005;184(1):63-9.
21 Roth CJ, Boll DT, Wall LK, Merkle EM. Evaluation of MRI acquisition workflow with lean six sigma method: case study of liver and knee examinations. AJR American journal of roentgenology. 2010;195(2):W150-6.
22 Martin DR, Sharma P, Kitajima H. Challenges and Clinical Value of Automated and Patient-Specific Dynamically Timed Contrast-Enhanced Liver MRI Examination. MAGNETOM Flash 2009; 3:40-5.
23 Breuer FA, Blaimer M, Mueller MF, et al. Controlled aliasing in volumetric parallel imaging (2D CAIPIRINHA). Magn Reson Med 2006, 55, 549-56.
24 Riffel P, Attenberger UI, Kannengiesser S, Nickel M, Arndt C, Meyer M, Schoenberg SO, Michaely HJ. Highly Accelerated T1-Weighted Abdominal Imaging Using 2-Dimensional Controlled Aliasing in Parallel Imaging Results in Higher Acceleration: A Comparison With Generalized Autocalibrating Partially Parallel Acquisitions Parallel Imaging. Investigative Radiology 2013: in press; DOI 10.1097/RLI.0b013e31828654ff.

Contact
Tobias Heye
University Hospital Basel
Department of Radiology
Petersgraben 4
CH-4031 Basel
Switzerland
Phone: +41 (0)61 328 6324
tobias.heye@usb.ch